

**A Bayesian inference framework for geomaterial characterization
and evaluation of complex soil-structure interactions**

Author

Jong, SC, Ong, DEL

Published

2024

Journal Title

Computers and Geotechnics

Version

Version of Record (VoR)

DOI

[10.1016/j.compgeo.2024.106452](https://doi.org/10.1016/j.compgeo.2024.106452)

Rights statement

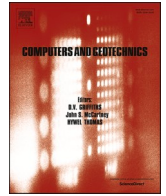
© 2024 The Author(s). Published by Elsevier Ltd. This is an open access article under the CC BY license (<http://creativecommons.org/licenses/by/4.0/>).

Downloaded from

<https://hdl.handle.net/10072/431375>

Griffith Research Online

<https://research-repository.griffith.edu.au>



Research Paper

A Bayesian inference framework for geomaterial characterization and evaluation of complex soil-structure interactions

S.C. Jong^{*}, D.E.L. Ong

Griffith University, School of Engineering and Built Environment and Cities Research Institute, Nathan, Queensland, Australia

ARTICLE INFO

Keywords:

Bayesian inference
 Bayesian regression
 Bayesian network
 Machine learning
 Geomaterials
 Soil-structure interactions

ABSTRACT

This research developed a robust Bayesian framework for evaluating geomaterials and soil-structure interactions involving deep excavation, utilizing Bayesian Regression and Bayesian Network methods that combined data training, validation, and updating into a cohesive framework. A methodology based on Bayesian Generalized Linear Model (a variant of Bayesian Regression) was applied to a laboratory-based case study on sustainable cementitious blends. The framework effectively used past research data to estimate design parameters even though the studies involved different mix design requirements. Then, a framework based on Gaussian Bayesian Network (a variant of Bayesian Network) incorporating Bayesian updating was applied to an established case history for deep excavation in clay. Two-dimensional finite element analysis was used to generate data for model training and updating. The GBN models accurately estimated responses such as wall deflections, wall bending moments, and ground surface settlements through a sequential updating process. The research was conducted using R programming language, with a custom R script designed to follow the process flow of the proposed framework. The successful application and validation of this framework demonstrated its potential for characterizing geomaterials and evaluating complex soil-structure interactions in deep excavation, leveraging on the availability of existing data and a reliable sequential updating process.

1. Introduction

The integration of Information Technology (IT) in data collection and analysis is a growing trend in the construction sector, leading to the application of artificial intelligence (AI) and machine learning (ML) in solving complex engineering problems. These techniques efficiently learn from data inputs and outputs, allowing for the identification of functional relationships that might be complex to interpret. AI models in this context are predominantly data-driven, relying heavily on data for model development, opposing traditional engineering-based methodologies that employ simplifying assumptions. Using ML, the data can be trained to create robust and effective design models, thus improving the engineering design process by reducing analysis time. These models also enhance problem understanding by analyzing complex relationships between various input parameters and yielding significant outputs, in contrast to traditional methods limited to low-dimensional engineering problems. In geotechnical engineering, ML applications cover a broad range including soil and rock characterization, foundations, slopes, tunnels, mining, liquefaction, and more, demonstrating their

capabilities in addressing a wide array of complex soil mechanics issues.

The complex behavior of geomaterials poses significant challenges in geotechnical engineering, as it complicates the understanding of their applications in construction projects. Engineering designs, often based on simplified principles, can misinterpret ground behavior due to these complexities. The variability of geological conditions adds uncertainty to geotechnical design, especially in understanding soil-structure interactions during complex underground construction (Ong et al., 2006; Ong, 2004). Being able to accurately quantify this uncertainty is key to enhancing the design of robust geotechnical structures. Traditional approaches involve extensive field and laboratory tests to comprehend the variable and uncertain ground conditions (Omeregic et al., 2019; Mehdizadeh et al., 2015), but these are hampered by high costs and large project scopes, leading to limited data availability. Conversely, continuous project monitoring generates extensive data, offering valuable insights but requiring substantial processing time. In this era of advanced technology, ML applications have emerged as solutions to these complex problems, addressing both the scarcity and abundance of data more effectively than traditional methods. The applications of ML

^{*} Corresponding author.

E-mail address: s.jong@griffith.edu.au (S.C. Jong).

<https://doi.org/10.1016/j.compgeo.2024.106452>

Received 20 January 2024; Received in revised form 24 April 2024; Accepted 18 May 2024

Available online 31 May 2024

0266-352X/© 2024 The Author(s). Published by Elsevier Ltd. This is an open access article under the CC BY license (<http://creativecommons.org/licenses/by/4.0/>).

techniques in geotechnical studies (Elbaz et al., 2019; Ghasemi and Gholizadeh, 2019; Hu and Wang, 2020; Hu et al., 2020; Jin et al., 2019; Pham et al., 2021; Pham et al., 2022; Kurnaz and Kaya, 2018) have led to an increasing emphasis on the use of common programming languages such as MATLAB (Phoon and Ching, 2014; Shams, 2024; Joaquin, 2024), Python (Walker, 2018; Stuyts, 2020), and R (Jong et al., 2022) in geotechnical engineering. These languages are particularly relevant for implementing ML techniques in geotechnical applications. They enable the processing and interpretation of large data sets, crucial for making informed decisions in geotechnical design and construction. This shift towards data-driven methodologies signifies a significant transformation in the field, moving away from reliance on empirical methods and towards a more nuanced understanding of the complex interactions in geotechnical systems.

An extensive review of the role of AI/ML in geotechnical research is available in Jong et al. (2021). Within these applications, Bayesian inference is particularly prominent for studying geomaterial properties (Yang et al., 2019; Zhao et al., 2019; Ching et al., 2017; Shi and Wang, 2021; Wang and Zhao, 2017; Gong et al., 2017). Its effectiveness arises from treating model parameters as probabilistic random variables rather than constants, as done in most ML methods, offering a more realistic reflection of their true nature (Ching and Phoon, 2019; Jin et al., 2018). Probabilistic method enables a reasonable quantification of prediction uncertainties, providing users with a measure of confidence in the model outputs, which aids in decision-making for future studies (Qi and Zhou, 2017). It is envisaged that the Bayesian method has a huge potential in addressing these problems to improve the understanding of the behavior of geomaterials and soil-structure interaction problems. This study thus aims to create a general framework based on Bayesian inference to study sustainable geomaterials and evaluate soil-structure interactions induced by deep excavations, by developing the capabilities for parameter estimation based on existing data and sequential updating with the acquisition of new data. A novel Bayesian inference framework will be developed using ML techniques and R programming language with the ability to consider complex relationships between input parameters and model outputs. Model parameters critical for geotechnical design will be inferred based on existing data available. The proposed method will provide an alternative to the preliminary study of new geomaterials and complement existing experimental and geotechnical design processes. Two established case studies collected from literature will be used to demonstrate the implementation of the proposed Bayesian framework for studying sustainable geomaterials and deep excavations respectively and its performance will be validated using collected laboratory/field data. By showcasing practical applications and demonstrating the efficacy of the proposed approach through these case studies, it is believed that this research could contribute meaningfully to enhance advanced methodologies within geotechnical engineering.

2. Overview of Bayesian Inference

The Bayesian inference is a method based on the principles of Bayes' theorem that deduces parameters and quantifies their uncertainties probabilistically (Murphy, 2012). Credible intervals (CIs) can thus be deduced from the probability distributions of the parameters, suggesting a range of plausible values for parameter estimates at a given level of credibility. According to Bayes' theorem, the posterior distribution of parameters, θ , given observed data, D , is denoted as $p(\theta|D)$, as described in Equation (1):

$$p(\theta|D) = \frac{p(\theta)p(D|\theta)}{p(D)} \quad (1)$$

where, $p(\theta|D)$ represents the posterior distribution of parameters, $p(\theta)$ is the prior distribution (existing knowledge before data observation), $p(D|\theta)$ is the likelihood function (probability of data given the model

parameters), and $p(D)$ is the model evidence, a normalizing factor.

The prior distribution integrates prior knowledge from sources like previous reports, field data, maps, surveys, and expert judgment (Wang and Cao, 2013). The model accommodates vague or non-informative priors in cases of high uncertainty or lack of prior information, making parameter estimates less dependent on priors. The likelihood function assesses the probability of observing the data given specific parameters, and the model evidence, integral to the model's normalization, is calculated by integrating the likelihood over all parameters as shown in Equation (2). Detailed methodology for developing a Bayesian model can be found in Houlsby and Houlsby (2013).

$$p(D) = \int p(\theta)p(D|\theta)d\theta \quad (2)$$

Since computing the integral in Equation (2) can be complex, sampling methods like Markov chain Monte Carlo (MCMC) simulations (Jin et al., 2018) are often employed. By applying Bayes' theorem, a Bayesian model infers parameters of interest probabilistically, combining prior knowledge from existing research with laboratory/field data available.

3. Proposed Bayesian Framework

A general, robust framework based on Bayesian inference was proposed in this research to study the behavior of geomaterials and evaluate soil-structure interactions by harnessing the powerful prediction capacity of ML-based techniques to process the complex relationships between various inputs and outputs. The Bayesian method is gaining increasing popularity for a wide range of applications in geotechnical engineering related to the fundamental understanding of geomaterial properties and ground behavior due to its superiority in back analyzing and updating design parameters crucial for geotechnical design. This novel study was thus motivated by the findings from the literature review to establish a general Bayesian framework that could be easily applied to different geotechnical studies. Therefore, the proposed Bayesian framework consists of two main capabilities: (i) estimation of desired output based on existing data and (ii) updating of desired output sequentially with new data acquired. Fig. 1 shows the general Bayesian framework proposed, in which two variants of the Bayesian method were employed, namely (i) Bayesian Regression and (ii) Bayesian Network, to develop the model that could estimate the strength of geomaterials as well as ground and wall responses induced by deep excavations, respectively.

The data for geomaterial characterization were collected from published and established study in the literature. A case study on sustainable cementitious blends for soft soil stabilization (Liu et al., 2022) was used to train and validate the applicability of the proposed Bayesian model to study geomaterials with different mix design requirements. The final model outputs obtained include a predictive equation that could be used for strength prediction of similar geomaterials and variable selection/model ranking (if assessment of the significance of inputs variables and their effects on the output is required). The successful model development would demonstrate its feasibility for application to the preliminary analysis of new geomaterials. On the other hand, two-dimensional (2D) finite element analysis (FEA) was conducted to generate the data required for training the proposed Bayesian Network model to estimate ground and wall responses induced by deep excavations. The FEA is a commonly used modeling technique in geotechnical engineering to study soil-structure interactions due to its user-friendliness and ability to conduct parametric studies to analyze the effects of different parameters on the ground and wall behavior (Chong, 2020). A commercially available finite element software, PLAXIS 2D (Bentley Systems, 2022) was used to carry out the numerical simulation of deep excavation in clay based on the case study (Ou et al., 2000) collected from the literature. The outputs obtained from the proposed Bayesian model include the profile predictions of wall deflection, wall bending moment and

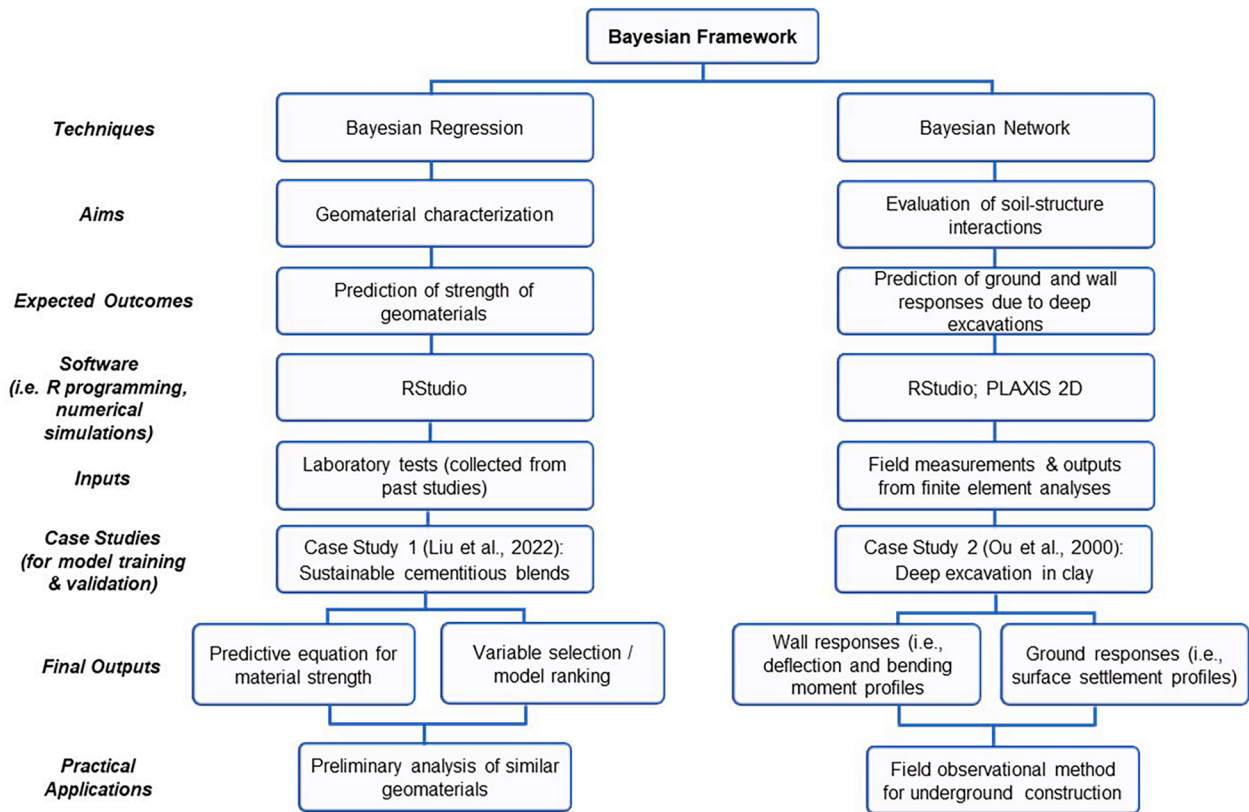


Fig. 1. Proposed general Bayesian framework for characterizing geomaterials and evaluating soil-structure interactions.

ground surface settlement. The successful implementation of the proposed model would prove its potential for application to underground construction works where field observational method is adopted.

3.1. Bayesian Regression

Prior to constructing a Bayesian model, data pre-processing is often necessary to enhance the model's consistency and efficiency. One common technique is data normalization, which adjusts input data to a uniform range, thereby balancing the influence of different variables and making their impacts on the output more uniform. As stated by Cheng et al. (2020), data from a dataset can be standardized using the 'min-max' scaler method, originally proposed by Masters (1993). This approach scales data to a predetermined minimum and maximum range, and in the absence of specified minimum and maximum values for scaling, the data will be adjusted to fall within the range of 0 to 1. In this study, a variant of Bayesian regression, the Generalized Linear Model (GLM), was employed for modeling the strength of geomaterials. Bayesian GLM is adept at accommodating various data structures (e.g., Normal, Poisson, Binomial, Negative Binomial, and Gamma probability distributions), offering a broader generalization capability compared to standard Bayesian regression models that are usually optimized for a single data structure type. The Bayesian GLM is generally expressed as:

$$g(E(Y)) = \beta_0 + \beta_1 X_1 + \dots + \beta_p X_p \quad (3)$$

where $E(Y)$ is the average Y value in the model and $g(\cdot)$ is the link function that is selected based on the data structure (i.e., type of probability distribution). For example, data comprising Normal distribution and ranging from 0 to $+\infty$ where log link function is used can be described as:

$$g(\mu_i) = \ln(\mu_i) = \beta_0 + \beta_1 X_{i1} + \dots + \beta_p X_{ip} \quad (4)$$

Utilizing a log link function ensures that when the predicted value is

reverted to its original scale, the predictors undergo exponentiation so that the values remain consistently positive. The training of the Bayesian model was conducted using Markov chain Monte Carlo (MCMC) simulation. The MCMC simulation is a technique that creates random samples of a parameter by forming a Markov chain that has the parameter's posterior distribution as its stationary distribution. This process involves drawing samples from estimated distributions and continually refining these estimates at each step, enhancing the accuracy until convergence is reached. It is important to diagnose the performance of the MCMC simulation to ensure that the sampling process has successfully converged to the desired posterior distribution and has operated efficiently without excessive computational time. One way to assess the efficiency of the simulation process is by examining a trace plot generated during the sampling process, which depicts the coefficient estimates for various parameters plotted against the number of iterations (see Fig. 2). According to Geyer (1992), an ideal chain exhibits rapid mixing, where the correlation between consecutive samples diminishes swiftly over time. Conversely, slow mixing suggests prolonged dependence among generated samples over numerous iterations. Fig. 2(a) depicts a scenario of slow mixing, characterized by significant fluctuations in the sampling process, indicating a longer time may be necessary for the chain to stabilize. In contrast, Fig. 2(b) illustrates rapid mixing, showcasing active simulation behavior in exploring the parameter space of the posterior distribution. To mitigate the impact of initial state fluctuations in the chain, a warm-up or burn-in period is typically employed, during which initial samples are discarded, and parameter estimates are derived from subsequent samples (Geyer, 1992). Additionally, conducting the sampling process through multiple independent, parallel Markov chains, each starting from different initial values but sharing the same length and burn-in samples, is recommended (Neal, 2011; Johnson et al., 2021). When rapid mixing occurs, trace plots from multiple chains should converge to the same posterior distribution, overlapping with each other (Murphy, 2012). The

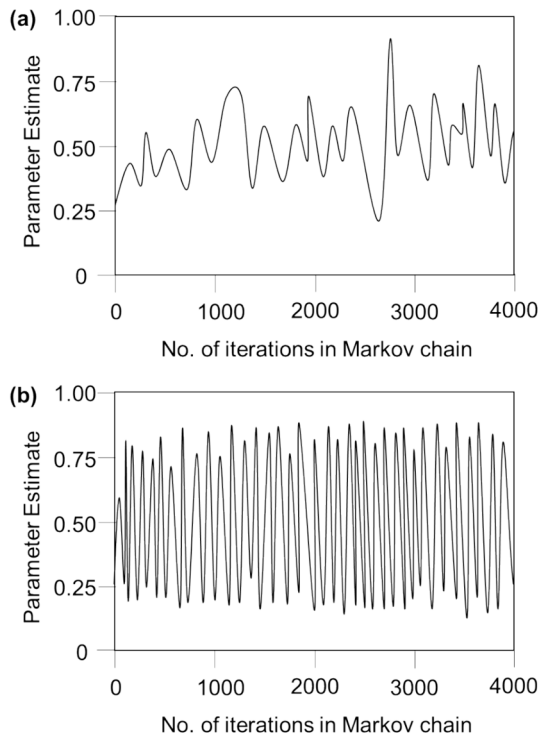


Fig. 2. Illustration of (a) slow mixing and (b) rapid mixing in the Markov chain during MCMC simulation.

Hamiltonian Monte Carlo (HMC) algorithm (Duane et al., 1987) is one of the commonly used MCMC algorithms that can sample from probability distributions more efficiently, and therefore adopted in this study. The details of HMC algorithms are described in Neal (2011) and Betancourt (2017).

To assess the model performance, a measure of model fit, the Bayesian R^2 (i.e., the Bayesian coefficient of determination), can be used. Furthermore, the normalized mean absolute error (NMAE) can be computed to measure the model residual error. The details of the computation of Bayesian R^2 and NMAE can be found in Gelman et al. (2019) and Jong et al. (2022), respectively. If the investigation of the importance of variables is required, the Bayesian variable selection process can be carried out to evaluate the significance of the variables by comparing the posterior probabilities of competing models that consist of random combinations of variables, so that the relative importance of model variables can be ranked accordingly. When new data are acquired, the Bayesian model can be updated by incorporating previous model output as prior into the model and repeating the modeling process, enabling the parameter estimates to be improved over time and subsequently reduces parameter uncertainties. Further details about the Bayesian variable selection and updating processes can be found in Jong et al. (2022).

3.2. Bayesian Network

A Bayesian Network is a graphical representation of a causal probabilistic network, depicted as a directed acyclic graph (DAG). In the DAG, nodes symbolize a collection of variables within the model, and directed edges connect the variables, indicating conditional dependencies between them (Khalaj et al., 2020). Consequently, the model can deduce causal links between variables using conditional probability distributions (Koski and Noble, 2009) and evaluate the impact of one variable on another throughout the learning process. The joint probability distribution of a Bayesian Network model can be expressed as:

$$P(a_1, a_2, \dots, a_n) = \prod_{i=1}^n P(a_i | Pa(a_i)) \quad (5)$$

where $Pa(a_i)$ is the parent set of variable a_i . A variant of Bayesian Network, the Gaussian Bayesian Network (GBN), was adopted in this study for model training since the data collected from 2D FEA for the study of deep excavation in clay consist of continuous variables. A GBN model comprises several Bayesian Regression models interconnected via conditional dependencies. These dependencies are symbolized by directed edges connecting all nodes in the model. Essentially, in the GBN structure, each node is associated with a locally developed regression model, which during the training phase, is connected to another node represented by a distinct regression model within the proposed Bayesian Network structure. Typically, constructing a Bayesian Network model involves two phases: (i) structure learning, which focuses on understanding the Bayesian Network structure, and (ii) parameter learning, which learns the nodes within the defined network structure. Given a Bayesian Network model, $B = (G, \Theta)$ where G denotes the structure and Θ denotes the parameters (i.e., nodes in the structure) with a given dataset D , the model learning process can be expressed as (Scutari and Denis, 2014):

$$Pr(B|D) = Pr(G, \Theta|D) = Pr(G|D) \bullet Pr(\Theta|G, D) \quad (6)$$

where $Pr(B|D) = Pr(G, \Theta|D)$ represents Bayesian Network learning, while $Pr(G|D)$ and $Pr(\Theta|G, D)$ represent structure learning and parameter learning, respectively. The model performance can be assessed using mean absolute error (MAE) and root mean square error (RMSE) (Pham et al., 2021; Pham et al., 2022; Leong et al., 2015). The MAE and RMSE are normalized using the range of the observed values so that the model errors can be evaluated on the same scale, with a value close to 0 being desirable, indicating that the model accuracy is high. Similar to Bayesian Regression, the Bayesian Network model can be updated whenever new data become available through the incorporation of previous output as prior into the model.

3.3. Implementation of the Proposed Bayesian Framework

The proposed Bayesian framework was implemented using R programming language (R Core Team, 2021) via the R-friendly editor RStudio (RStudio Team, 2021). Original R codes were developed to carry out the implementation process by applying the proposed framework to established case studies to assess the feasibility of the Bayesian inference method. In this study, some libraries readily available in RStudio were used to develop the proposed models based on Bayesian Regression and Bayesian Network and plot the graphical results, including *rstanarm* (Goodrich et al., 2020), *bnlearn* (Scutari, 2010), *ggplot2* (Wickham, 2016) and *bayesplot* (Gabry and Mahr, 2021). Further details about the implementation process of the proposed methodology are provided in the supplementary material.

4. Application to Case Studies

4.1. Case Study 1 – Study on Sustainable Cementitious Blends (Liu et al., 2022)

The proposed Bayesian Regression framework was applied to a published case study to examine its feasibility. Liu et al. (2022) evaluated sustainable geomaterials for soft soil stabilization, aiming to decrease cement usage in construction by partially substituting Ordinary Portland Cement (OPC) in conventional cement-only mixes. Their study focused on two types of sustainable cementitious blends: (i) fly ash-blended cement and (ii) DuraCrete-blended cement. These materials were explored as alternatives to reduce the amount of OPC needed for soil stabilization. DuraCrete, composed of mineral oxides and alkaline-

based materials, offers a significantly lower carbon dioxide emission level than OPC, as it does not require energy-intensive processes, making it as a sustainable option for soil stabilization. Liu et al. (2022) assessed the viability of using fly ash and DuraCrete as partial OPC replacements through a series of lab tests to understand the behavior of soft soil samples stabilized with three types of binders: (i) OPC only (for baseline comparison), (ii) fly ash-blended cement, and (iii) DuraCrete-blended cement. These soil specimens were created using soft marine clay collected from the Port of Brisbane, Australia, with moisture contents as high as 130 %. The Unconfined Compressive Strength (UCS) of these specimens was examined, with 20 sets of stabilized soil specimens prepared for each binder type, featuring total mixture contents of 10, 15, 20, 25, and 30 %. For each mixture content, fly ash to cement ratios of 1:1, 1:2, 1:3, and 1:4 were used, while DuraCrete to cement ratios were 3:100, 5:100, 7:100, and 9:100. In total, Liu et al. (2022) gathered 25 datasets from their study for specimens stabilized using fly ash-blended cement and DuraCrete-blended cement, respectively (i.e., 5 datasets from the baseline study plus 20 datasets from each blended cement study).

In this study, the proposed Bayesian Regression methodology was employed to predict the UCS of soil specimens stabilized with two distinct types of cementitious blends to investigate the ability of the proposed Bayesian model to adapt to various data observations. The process involved initially training the model with datasets from fly ash-blended cement, followed by validation using datasets from DuraCrete-blended cement. Due to the differences in mixture components and designs between the two binders, the model would be validated using totally independent validation data, allowing the generalization capability of the developed model to be assessed. Table 1 summarizes the factors considered in the proposed Bayesian model and the statistical parameters for both types of cementitious blends. Four key factors were considered in the model for predicting the strength of the stabilized soil specimens. For fly ash-blended cement, these were cement content (C), fly ash content (F), total water content (W), and the water to cement blend ratio (W/b). In the case of DuraCrete-blended cement, the model included similar factors, but with DuraCrete content (DC) substituting for fly ash content (F). Notably, the range of cement and binder contents differed across the datasets, reflecting the varied mixing ratios used in their designs. All datasets were pre-processed before training process, and a log link function was used in the Bayesian model. Consequently, the Bayesian model developed for fly ash-blended cement is expressed as:

$$\ln(\text{UCS}) = \beta_0 + \beta_1 C + \beta_2 F + \beta_3 W + \beta_4 (W/b) \tag{7}$$

Where $\beta = (\beta_1, \beta_2, \beta_3, \beta_4)$ denotes the vector of unknown parameters (i.e., coefficients for the input variables) to be estimated by the developed model.

4.1.1. Results and discussion

The Bayesian model was trained using MCMC simulation, employing

five parallel Markov chains to ensure convergence. Each chain generated 10,000 samples, of which 50 % were discarded as burn-in samples, resulting in 25,000 samples for parameter estimation across various model variables. Thus, the sampling process involved the construction of five parallel Markov chains, each comprising 5,000 samples for parameter estimation. The mean coefficient estimates as well as the 85 % and 95 % credible intervals (CIs) obtained from the model are summarized in Table 2. Based on the parameter estimates, the equation for predicting the strength of fly ash-blended cement is formulated as:

$$\ln(\text{UCS}) = -1.781 + 1.193C - 0.391F + 0.617W - 1.825(W/b) \tag{8}$$

The model was subsequently validated using data from DuraCrete-blended cement studies. Fig. 3 displays a comparison between the actual and predicted UCS for both fly ash-blended cement (training phase) and DuraCrete-blended cement (validation phase).

As shown in Fig. 3(a), the model accurately predicted the strength of soil specimens stabilized with fly ash-blended cement, evident from the close alignment of predicted values with measured ones and the narrow CIs. However, during the generalization to different data with a similar material design (see Fig. 3(b)), the model maintained a good accuracy, but with increased prediction uncertainty, indicated by broader CIs, especially for dataset numbers 10, 15, 20, 24, and 25. Notably, the model inaccurately predicted for dataset numbers 5 and 9 in the validation phase, where the predicted values and their 85 % CIs failed to encompass the actual UCS values. When comparing UCS values of soil specimens stabilized with fly ash and DuraCrete-blended cement, it was noted that fly ash-blended cement specimens generally exhibited lower strength in lab tests compared to those made with DuraCrete-blended cement, despite using identical total mixture contents.

Liu et al. (2022) found that incorporating DuraCrete into the cementitious blends significantly enhanced the strength of stabilized soft soils. This increased strength in DuraCrete-stabilized specimens was attributed to better cementation bonding, leading to a denser structure and higher strength due to more effective bonding between soil particles. Conversely, increased fly ash content in cementitious blends led to reduced cement hydration and lower strength. As a result, when the model was initially trained with datasets showing lower UCS values, it required extrapolation during validation with datasets that exhibited

Table 2

Output summary of mean parameter estimates and credible intervals for fly ash-blended cement (model training).

Variables (X_p)	Parameters (β_p)	Mean Estimate Values	85 % Credible Intervals	95 % Credible Intervals
(Intercept)	β_0	-1.781	[-2.52, -1.05]	[-2.77, -0.76]
C	β_1	1.193	[-1.03, 3.44]	[-1.83, 4.25]
F	β_2	-0.391	[-1.73, 0.96]	[-2.22, 1.44]
W	β_3	0.617	[-1.18, 2.40]	[-1.80, 3.02]
W/b	β_4	-1.825	[-2.77, -0.93]	[-3.16, -0.62]

Table 1

Factors considered in the Bayesian Regression model and statistical parameters for: (i) fly ash-blended cement and (ii) DuraCrete-blended cement.

Factors		Unit	Notation	Minimum	Maximum	Mean	Range	Standard Deviation
(i) Fly ash-blended cement								
Inputs	Cement content	%	C	5.0	30.0	14.9	25.0	6.4
	Fly ash content	%	F	0	15.0	5.1	15.0	4.0
	Total water content	%	W	135.0	145.0	140.0	10.0	3.6
	Water/cement blend ratio	-	W/b	4.8	13.5	8.0	8.7	3.2
Output	UCS of stabilized soft soil specimens	kPa	UCS	34.6	887.4	258.8	852.8	216.5
(ii) DuraCrete-blended cement								
Inputs	Cement content	%	C	9.1	30.0	19.1	20.9	6.9
	DuraCrete content	%	DC	0	2.7	1.0	2.7	0.8
	Total water content	%	W	135.0	145.0	140.0	10.0	3.6
	Water/cement blend ratio	-	W/b	4.8	13.5	8.0	8.7	3.2
Output	UCS of stabilized soft soil specimens	kPa	UCS	64.5	960.7	369.7	896.2	285.7

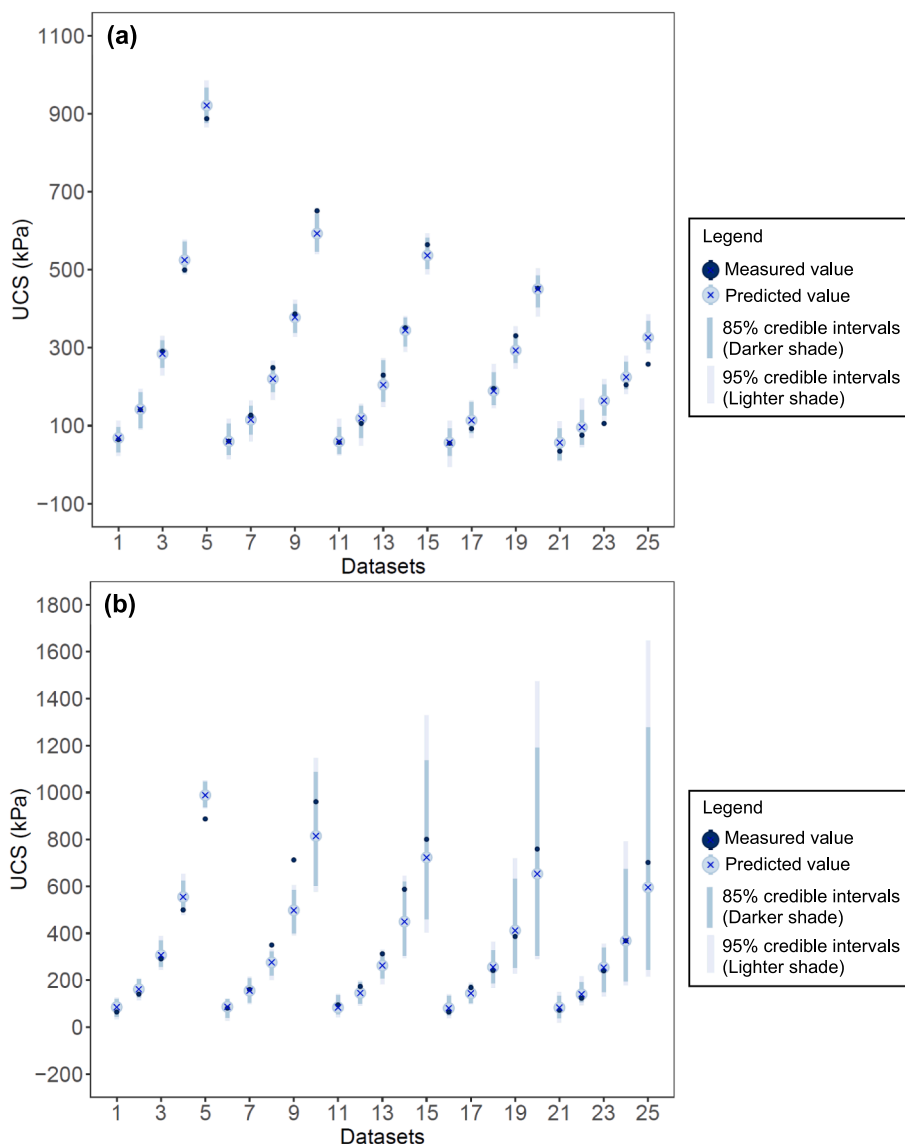


Fig. 3. Comparison of measured vs. predicted unconfined compressive strength (UCS) of stabilized soft soil specimens for: (a) fly ash-blended cement (model training) and (b) DuraCrete-blended cement (model validation).

higher UCS values. This led to a decrease in the model’s overall predictive accuracy and an increase in uncertainty, as the model needed to adjust to new datasets with values extending beyond those encountered during its initial learning phase.

Additionally, the mapping between the predicted and measured UCS of stabilized soil specimens and various factors for both types of cement blends is depicted in Figs. 4 and 5. Analysis of these figures reveals that the model accurately predicted soil specimen strength, particularly when factoring in total water content (W) and the water to cement blend ratio (W/b). This was attributed to the use of consistent ranges for these factors in both fly ash and DuraCrete cement blends. In terms of cement content, the model predictions remained accurate, as both blends had a similar cement content range: 5 to 30 % for fly ash-blended cement and 9.1 to 30 % for DuraCrete-blended cement. However, the accuracy in mapping predicted to measured UCS values was less accurate when considering the DuraCrete content (DC), as illustrated by the larger discrepancies in Fig. 5(b) compared to Fig. 4(b). This variance was due to the narrower range of DuraCrete content (0 to 2.7 %) used by Liu et al. (2022), compared to the broader range used for fly ash content (0 to 15 %). The maximum DuraCrete content was significantly lower than the maximum fly ash content, leading to more significant differences in

model predictions during validation due to the interpolation required for adapting to new datasets with smaller ranges.

Figs. 4 and 5 demonstrate the ability of the developed Bayesian model to accurately depict the relationships between the strength of stabilized soils and key factors like cement content and water to binder ratio, which are crucial for strength development in soils stabilized with cementitious materials (Horpibulsuk et al., 2010). As shown in Fig. 4(a) and 5(a), an increase in cement content (C) led to higher UCS in specimens, aligning with the enhanced bonding between soil particles at higher cement concentrations (Horpibulsuk et al., 2010). This observation was consistent with other research findings in soil stabilization using cementitious materials (Pham et al., 2021; Pham et al., 2022). Fig. 4(d) and 5(d) show a decrease in predicted strength with an increase in the water to cement blend ratio (W/b), corroborating results from Liu et al. (2022). This demonstrates that the model could make accurate predictions and accurately capture the relationships between the strength of stabilized soils with different sustainable cementitious blends and various factors influencing strength development. Table 3 summarizes the model performance in terms of fitting and error metrics for predicting the strength of specimens stabilized with two different binders.

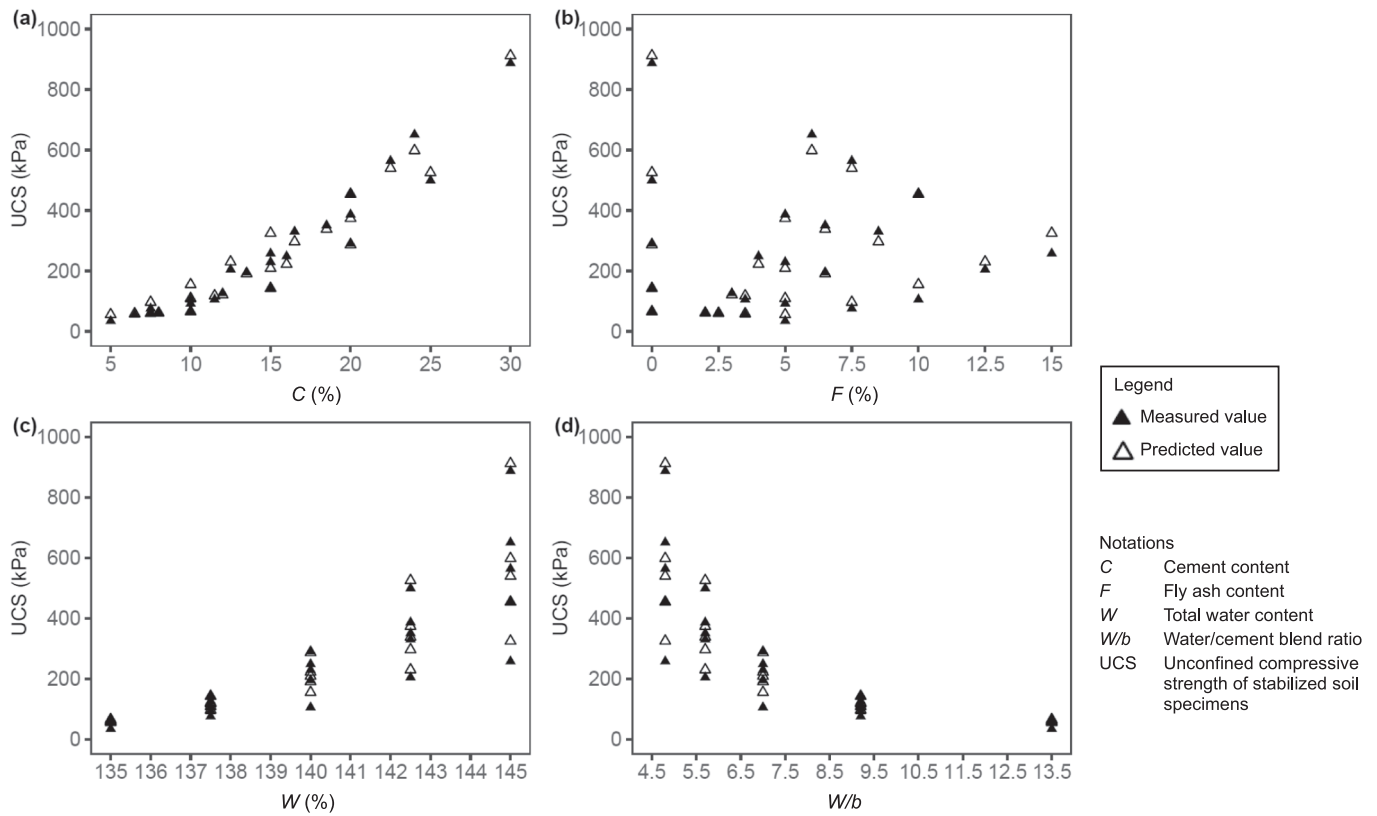


Fig. 4. Mapped measured and predicted unconfined compressive strength (UCS) of soil specimens stabilized with fly ash-blended cement vs. the factors considered (model training).

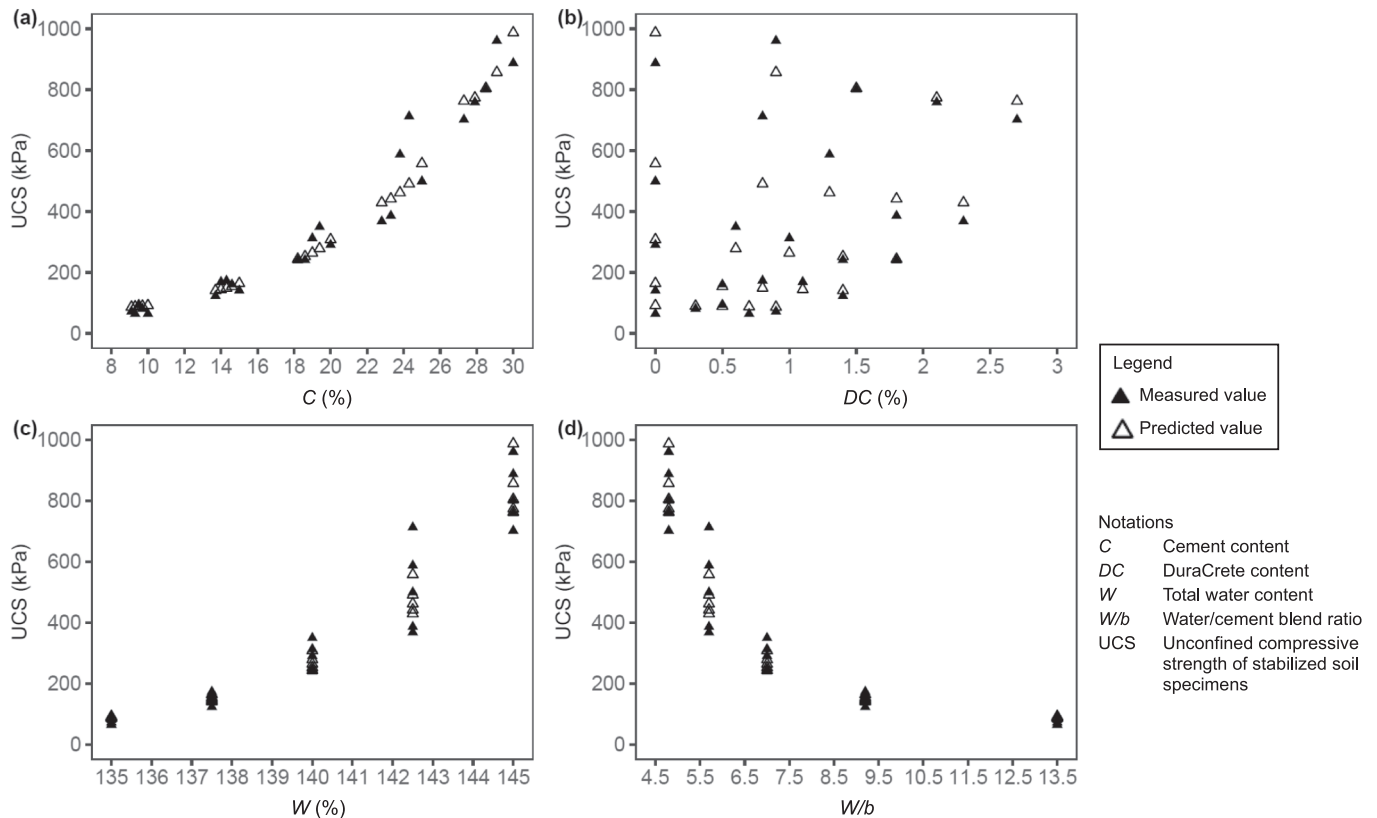


Fig. 5. Mapped measured and predicted unconfined compressive strength (UCS) of soil specimens stabilized with DuraCrete-blended cement vs. the factors considered (model validation).

Table 3
Summary of model performance for fly ash-blended cement (training) and DuraCrete-blended cement (validation).

Stages	Training (Fly ash-blended cement)	Validation (DuraCrete-blended cement)
Bayesian R^2	0.9854	0.9313
NMAE	0.0730	0.1224
Proportion ¹ of observed values within 85 % prediction intervals (out of 1)	0.88	0.88
Proportion ¹ of observed values within 95 % prediction intervals (out of 1)	0.96	0.88

¹ A proportion of 1 indicates that the model can capture 100% of the observed values within the prediction intervals.

The model exhibited a lower prediction accuracy for DuraCrete-blended cement (Bayesian $R^2 = 0.9313$ and NMAE = 0.1224) than for fly ash-blended cement (Bayesian $R^2 = 0.9854$ and NMAE = 0.0730). Despite this, both models successfully captured the same proportion of observed values within their 85 % prediction intervals (proportion = 0.88). A larger proportion of observed values fell within the 95 % prediction intervals during training (proportion = 0.96) compared to validation stage (proportion = 0.88), indicating that the model could be generalized to analyze different types of data with reasonable accuracy.

4.2. Case Study 2 – Construction of Taipei National Enterprise Center (TNEC), Taiwan (Ou et al., 2000)

The well-documented Taipei National Enterprise Center (TNEC) project in Taiwan was adopted as the case study to evaluate soil-structure interactions induced by deep excavation in clay using the proposed Bayesian Network framework. Fig. 6 illustrates the subsurface soil profile and the typical cross-section of the TNEC excavation.

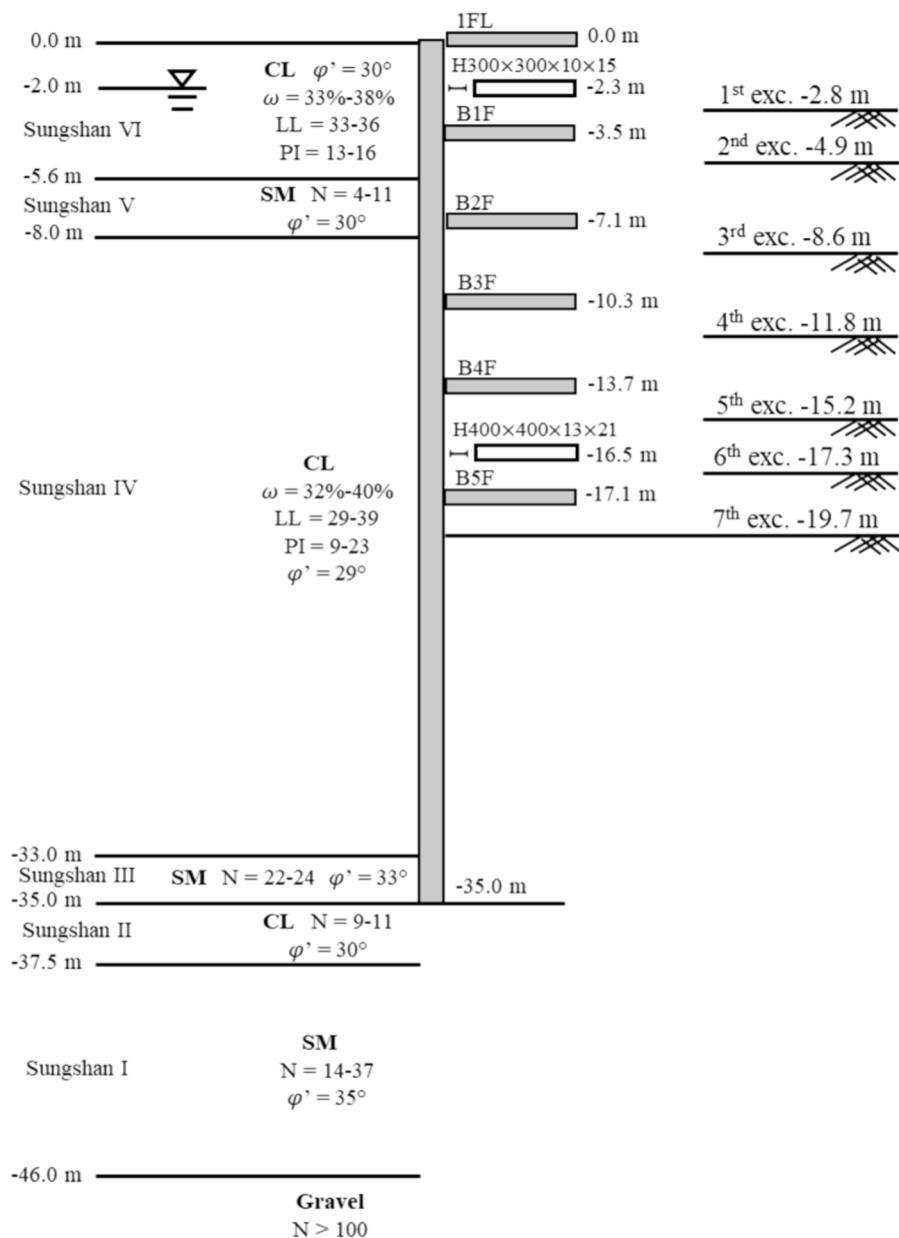


Fig. 6. The subsurface soil profile and typical cross-section for deep excavation for TNEC, Taiwan (adapted from Lim and Ou (2017)).

The excavation dimensions for the TNEC construction were 43 m wide and 106 m long on the south side, extending to 61 m on the north. Executed in seven stages to a depth of 19.7 m, the excavation used the top-down construction method, supported by 0.9 m thick, 35 m deep diaphragm walls, as outlined in the construction sequence in Table 4.

This study employed the Hardening Soil model for effective stress undrained (Undrained (A)) and drained analysis to simulate soft silty clay and silty sand, respectively (Lim and Ou, 2017). Tables 5 and 6 summarize the soil and structural properties employed in the 2D FEA to generate training data for the proposed Bayesian Network model.

For silty fine sand layers, stiffness values were calculated, with tangent stiffness for primary oedometer loading (E_{oed}^{ref}) set at $1E_{50}^{ref}$ and unloading/reloading stiffness (E_{ur}^{ref}) at $3E_{50}^{ref}$, as per the PLAXIS 2D Material Models Manual (2022). The power (m) values of 0.5 for sand (Schanz et al., 2000) and 1.0 for clay (Lim and Ou, 2017) were used. The dilatancy angle (ψ) was set to $\phi - 30^\circ$, and a Poisson's ratio for unloading-reloading (ν_{ur}) of 0.2 was applied (Lim and Ou, 2017). For the diaphragm wall, Young's modulus (E) of 21E6 kPa and a Poisson's ratio of 0.15 (Lim and Ou, 2017) were adopted in the numerical model. To account for concrete cracking, structural member stiffnesses were reduced by 20 % from nominal values (Lim and Ou, 2017).

Fig. 7(a) shows the computed wall deflections from the developed finite element model (FEM) closely aligning with field measurements, displaying cantilever wall deformations in the initial excavation stage and deeper inward lateral movements at greater depths, consistent with trends described by Clough and O'Rourke (1990) for braced excavations. In Fig. 7(b), the numerical model accurately predicted ground surface settlements, particularly after reaching the fifth excavation stage, despite earlier stages showing larger computed settlements than observed. Fig. 7(c) presents the wall bending moment profiles from the 2D FEA. As bending moments are derived from wall deflection curvature, they exhibit trends similar to the deflection profiles. The maximum positive bending moments occurred near the excavation levels for each stage, while the maximum negative moments were consistently found at a depth of 3.5 m from the surface, corresponding to the B1F floor slab installation location. The close mapping of the FEA outputs with the field data reported by Ou et al. (2000) indicates that the numerical results are reliable for training the proposed GBN model. For each excavation stage, a total of 145 datasets were gathered, detailing computed wall deflection and wall bending moment profiles, while 124 datasets per stage were derived from the FEA outputs for ground settlement profiles.

Design parameters including (i) secant stiffness (from drained

Table 4
Summary of construction sequence for TNEC, Taiwan (after Kung et al. (2009)).

Stages	Construction Activities
0	Constructed diaphragm walls, pile foundation
1	Excavated to elevation -2.8 m
2	Installed steel strut 1 (H300 × 300 × 10 × 15) at elevation -2.0 m (preload = 784.8 kN per prop)
3	Excavated to elevation -4.9 m
4A	Cast floor slab (B1F) at elevation -3.5 m
4B	Removed steel strut 1 and cast ground level of slab (1FL)
5	Excavated to elevation -8.6 m
6	Cast floor slab (B2F) at elevation -7.1 m
7	Excavated to elevation -11.8 m
8	Cast floor slab (B3F) at elevation -10.3 m
9	Excavated to elevation -15.2 m
10	Cast floor slab (B4F) at elevation -13.7 m
11	Excavated to elevation -17.3 m (center strip)
12	Installed steel strut 2 (H400 × 400 × 13 × 21) at elevation -16.5 m (preload = 1,177 kN per prop)
13	Excavated to elevation -19.7 m
14	Cast foundation slab
15	Cast floor slab (B5F) at elevation -17.1 m
16	Removed steel strut 2

triaxial test (E_{50}^{ref}), (ii) c' and ϕ' (from drained triaxial test, direct shear test or available site investigation reports), and (iii) retaining wall's depth (z) (from routine deep excavation design process), were utilized as inputs. For estimating ground surface settlements, the same soil parameters (E_{50}^{ref} , c' and ϕ') and the distance from the retaining wall (x) were used, rather than the wall's depth. The Bayesian Network models were trained stage-by-stage through the parameter learning process until reaching the final excavation stage. A similar deep excavation study in clay, reported by Korff (2013) for the construction of Ceinturbaan Station in Amsterdam, was used for the Bayesian updating process in this study. Both studies were independent of each other but similar in the sense of having seven excavation stages using the top-down construction method. During the learning phase for the initial excavation stage, the GBN model developed for studying TNEC excavation integrated the FEA outputs from the first excavation stage of Ceinturbaan Station excavation as prior knowledge.

In the initial stage, the GBN model thus incorporated five input parameters: E_{50}^{ref} , c' , ϕ' , z and $\delta_{h,1st(prior)}$, to learn the soil parameters and FEA wall deflection outputs to predict the wall deflection profiles, expressed as:

$$\text{GBN Model}_{1st,upd} = [\delta_{h,1st} | z, E_{50}^{ref}, c', \phi', \delta_{h,1st(prior)}] \quad (9)$$

where $\delta_{h,1st(prior)}$ denotes the wall deflection data from an independent study (prior knowledge) and $\delta_{h,1st}$ denotes the estimated wall deflections at the first excavation stage (also considered as the child of nodes " z ", " E_{50}^{ref} ", " c' ", " ϕ' ", and " $\delta_{h,1st(prior)}$ " in the model). The model was updated for the subsequent stages by carrying forward the outputs from the initial stage to the next and repeating the learning process, thereby expanding the GBN structure. The inclusion of past training results into the model helps maintain earlier learnings and enhances the accumulated knowledge in the model. The model was thus progressively trained at each stage of the excavation, deepening its insights by utilizing the outcomes from one stage as inputs for the next, ensuring continuous model refinement and updating. Upon reaching the final excavation depth, the GBN model was updated to:

$$\text{GBN Model}_{final} = [\delta_{h,n} | z, E_{50}^{ref}, c', \phi', \delta_{h,n-1}] \cdots [\delta_{h,3rd} | z, E_{50}^{ref}, c', \phi', \delta_{h,2nd}]$$

$$[\delta_{h,2nd} | z, E_{50}^{ref}, c', \phi', \delta_{h,1st}] [\delta_{h,1st} | z, E_{50}^{ref}, c', \phi', \delta_{h,1st(prior)}] \quad (10)$$

where n denotes the number of excavation stages in the study. The wall bending moments and ground surface settlements were estimated using the same parameter learning process, based on their respective training datasets obtained from 2D FEA.

4.2.1. Results and discussion

The profiles of wall bending moment, wall deflection and ground surface settlement estimated using the proposed Bayesian framework are presented and discussed hereinafter.

Fig. 8 presents the wall deflection profiles estimated by the GBN model for the TNEC excavation, compared with field measurements from Ou et al. (2000) for straightforward comparison of the model predictions with actual data. The model accurately predicted wall deflections from the earliest to the final excavation stages after incorporating data from a similar study (Korff, 2013) as prior knowledge during the updating process. The results clearly demonstrates the efficacy of the Bayesian updating process in this study. Applying the same learning approach but incorporating prior knowledge at the outset significantly enhanced the model's understanding of excavation-induced wall deformations. This knowledge was then extended to subsequent stages up to the final excavation. With the prior information as a new input, the model adeptly learned the initial cantilever wall deformations and subsequently improved its predictions for deep inward wall movements

Table 5
Summary of soil properties for TNEC, Taiwan (after Lim and Ou (2017)).

Soil Type	Soil Layer	Depth (m)	γ_r (kN/m ³)	c' (kPa)	ϕ' (°)	E_{50}^{ref} (kPa)	E_{oed}^{ref} (kPa)	E_{ur}^{ref} (kPa)	K_0	OCR
Soft silty clay	1-a	0 – 2	18.25	0	30	7,033	4,923	21,100	1.00	4
	1-b	2 – 4	18.25	0	30	6,826	4,779	20,479	1.00	4
	1-c	4 – 5.6	18.25	0	30	6,631	4,642	19,894	1.00	4
Loose silty fine sand	2	5.6 – 8	18.93	0	30	34,175	34,175 ¹	102,525 ¹	0.50	–
Soft silty clay	3-a	8 – 12	18.15	0	29	8,521	5,964	25,562	0.59	1.4
	3-b	12 – 16	18.15	0	29	9,526	6,668	28,578	0.56	1.25
	3-c	16 – 20	18.15	0	29	9,620	6,734	28,860	0.56	1.25
	3-d	20 – 24	18.15	0	29	9,290	6,503	27,870	0.56	1.25
	3-e	24 – 27	18.15	0	29	9,049	6,335	27,148	0.55	1.23
	3-f	27 – 30	18.15	0	29	9,158	6,410	27,474	0.55	1.23
	3-h	30 – 33	18.15	0	29	8,935	6,255	26,806	0.55	1.23
Medium dense silty fine sand	4	33 – 35	19.62	0	33	132,736	132,736 ¹	398,208 ¹	0.45	–
Medium soft clay	5	35 – 37.5	19.13	0	30	10,016	7,011	30,049	0.50	1
Medium dense to dense silt / silty fine sand	6	37.5 – 46	19.62	0	35	150,123	150,123 ¹	450,369 ¹	0.43	–

¹ Calculated in the finite element analysis.

Table 6
Summary of structural properties used for anchors (after Lim and Ou (2017)).

Anchor	Spacing (m)	Thickness (m)	Cross-sectional area (m ²)	Young's modulus, E (kPa)	ν
Steel strut 1	8	–	0.012	21E7	0.15
Steel strut 2	3.4	–	0.0219	21E7	0.15
Concrete slab	–	0.15	–	21E6	0.15

typical in braced excavations with multiple lateral supports. Thus, the model could accurately learn both types of lateral wall movements commonly observed in deep excavations, aligning with established findings in the field (Clough and O'Rourke, 1990; Hsieh and Ou, 1998; Likitlersuang et al., 2019).

Fig. 9 displays the estimated wall bending moment profiles derived using the same updating process. Mirroring the findings for wall deflection profiles, the GBN model adeptly replicated the wall responses, accurately reflecting the changes in both positive and negative bending moments throughout all excavation stages. These changes corresponded with the types of wall deformations observed and the positioning of

lateral supports at increasing excavation depths. Introducing prior knowledge from a similar study right at the first excavation stage allowed the model to learn about expected wall behavior. The learned information was carried through subsequent stages, enhancing the updating process as additional data became available. Consequently, the ability of the model to make accurate inferences and parameter estimations based on existing data was significantly improved, ensuring precise estimations of the desired outputs.

Fig. 10 shows the estimated ground surface settlement profiles for the TNEC excavation. Incorporating prior data from a similar study during the updating process improved the ability of the model to learn the 'spandrel type' ground settlement profile, which typically occurs due to cantilever wall deformations in the early stages of excavation. This happens when diaphragm walls act flexibly because of either the absence of lateral supports or inadequate preload for excavation support, as noted by Clough and O'Rourke (1990). This is evident in Fig. 10 (a) and (b), where the ground settlement profiles are identified as 'spandrel type', with maximum surface settlement occurring behind the retaining wall and diminishing with increasing distance from the wall. As excavation progressed, the model accurately tracked the transition from 'spandrel type' to 'concave type' ground settlements, reflecting the impact of lateral supports in countering soil pressure behind the diaphragm wall. Throughout the excavation stages, the model maintained high accuracy in estimating ground settlements, accurately recognizing

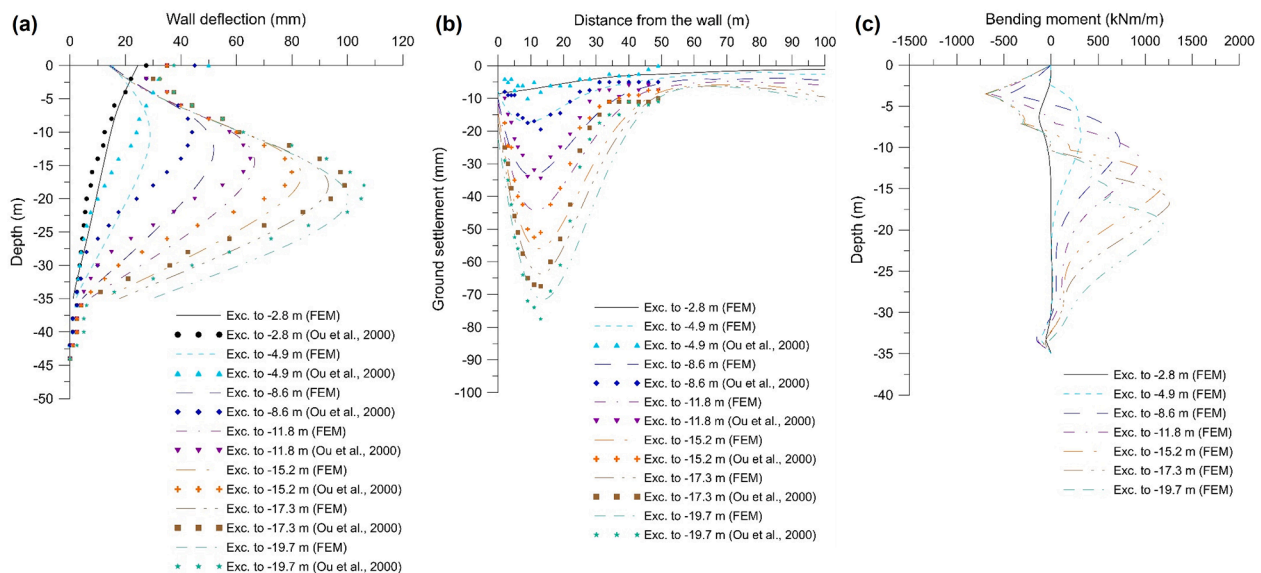


Fig. 7. Compiled PLAXIS 2D outputs for simulating the deep excavation for TNEC, Taiwan: (a) wall deflection profiles, (b) ground surface settlement profiles, and (c) wall bending moment profiles.

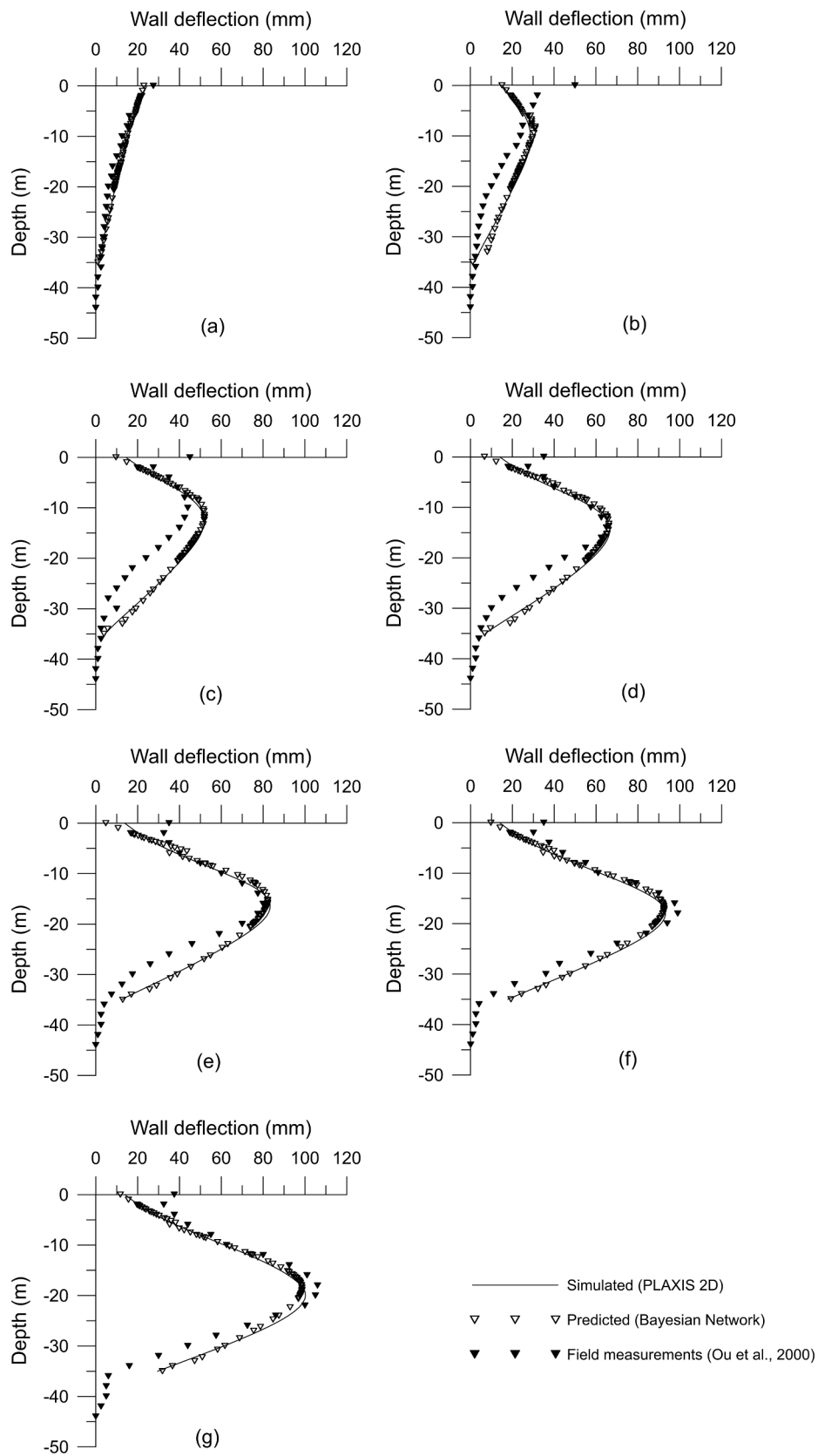


Fig. 8. Simulated and estimated wall deflection profiles with field measurements for TNEC, Taiwan for the excavation depths: (a) 2.8 m, (b) 4.9 m, (c) 8.6 m, (d) 11.8 m, (e) 15.2 m, (f) 17.3 m, and (g) 19.7 m.

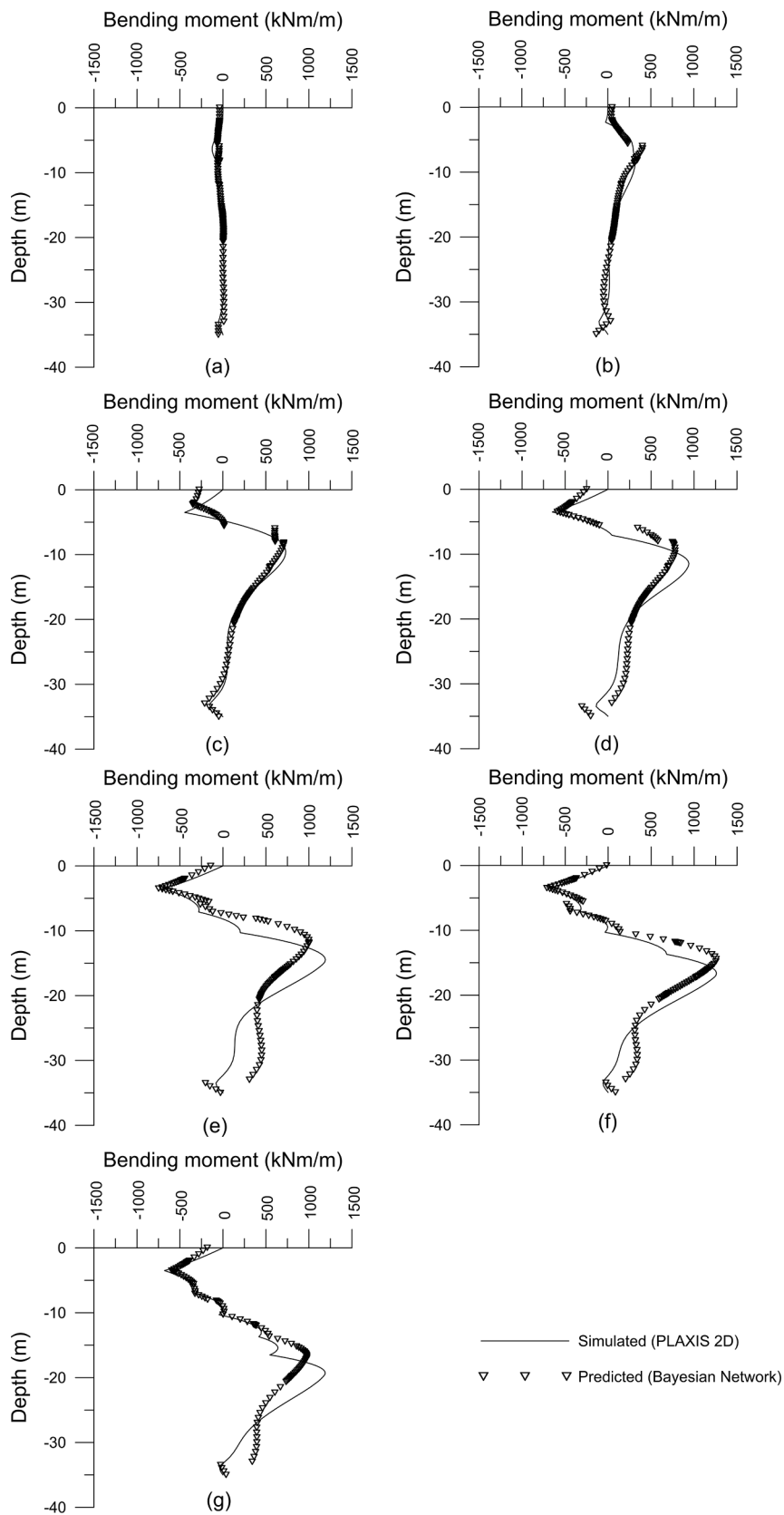


Fig. 9. Simulated and estimated wall bending moment profiles for TNEC, Taiwan for the excavation depths: (a) 2.8 m, (b) 4.9 m, (c) 8.6 m, (d) 11.8 m, (e) 15.2 m, (f) 17.3 m, and (g) 19.7 m.

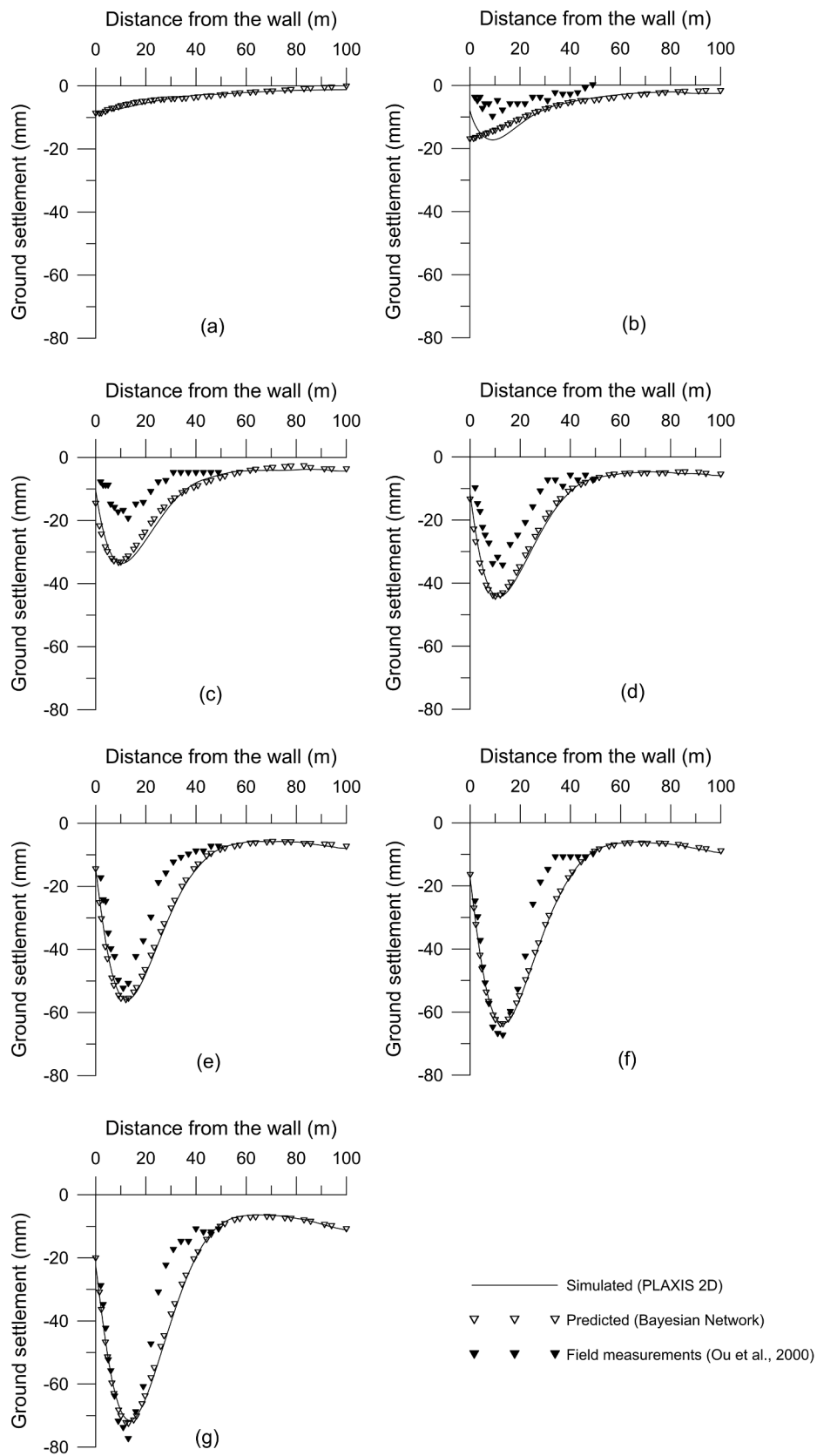


Fig. 10. Simulated and estimated ground surface settlement profiles with field measurements for TNEC, Taiwan for the excavation depths: (a) 2.8 m, (b) 4.9 m, (c) 8.6 m, (d) 11.8 m, (e) 15.2 m, (f) 17.3 m, and (g) 19.7 m.

both ‘spandrel type’ and ‘concave type’ profiles typically seen in multi-stage braced excavations (Clough and O’Rourke, 1990; Hsieh and Ou, 1998; Likitlersuang et al., 2019). By the end of the updating process, the developed GBN model had successfully inferred necessary parameters and produced precise model outputs, demonstrating its capability in identifying diverse ground settlement patterns.

Fig. 11 presents the evaluation of the model performance for the study of deep excavation in clay, utilizing NMAE and NRMSE, calculated for each excavation stage. The highest model error was observed at the first excavation stage for wall bending moment profile estimations (NMAE = 0.1462; NRMSE = 0.1990). The estimation of ground settlement profiles followed (NMAE = 0.0578; NRMSE = 0.0675), while wall deflection profile estimations yielded the lowest error (NMAE = 0.0117; NRMSE = 0.0146). As the excavation progressed deeper, the model error decreased progressively, reflecting an improvement in model accuracy. Upon comparing the model performance from the initial to the last excavation stages, a notable reduction in error was observed for all profile estimations. The decrease in model error was attributed to the integration of prior knowledge from the previous stage to the next, enhancing the efficiency of parameter learning.

4.3. Advantages and Limitations of the Proposed Methodology

The results from two case studies affirm the efficacy of the proposed Bayesian methodology in predicting the strength of sustainable geomaterials with varying mixtures in a laboratory setting, considering different aggregates, binders, proportions, and mixing conditions. The proposed Bayesian approach provides a probabilistic model that quantifies uncertainty in predictions alongside providing estimated values. The developed Bayesian model that is easy to interpret and update with new information, can serve as a predictive tool in future studies. Crucially, the Bayesian updating process allows for incorporating earlier results, retraining the model with new datasets, and saving computational time. Supply of the prior data could enhance the adaptability and accuracy of the model at subsequent project stages, leading to more reliable predictions. The robustness of the model for generalization was validated by using independent datasets from different studies,

demonstrating its capability to maintain accuracy across varied data types. This underscores the feasibility of the proposed approach for application to other geotechnical problems, though caution is advised, particularly when extrapolating to new data types or significantly different geomaterial properties. In terms of practical application, the Bayesian framework shows promise in evaluating soil-structure interactions during deep excavations. The model could refine its parameter inferences and deformation estimations through sequential updates, as evidenced by the case study. Its ability to integrate learned outputs from previous stages makes it adaptable for projects with evolving field data, contributing to economical and safe construction designs. The wealth of existing deep excavation case histories also offers a rich data source for enhancing the Bayesian model, further expanding its application in geotechnical engineering.

5. Conclusions

A Bayesian inference framework based on Bayesian Regression and Bayesian Network has been developed to study sustainable geomaterials and soil-structure interactions in deep excavations. The proposed framework has demonstrated its feasibility, robustness, and applicability in complementing existing laboratory and geotechnical design processes, offering a viable tool for the preliminary analysis of geotechnical problems. The successful application of the Bayesian framework to two established case studies collected from the literature further demonstrates the implementation and validation of the proposed methodology in this study. The significant findings from this study are concluded as follows:

- The Bayesian GLM accurately predicted the strength of stabilized soils, quantifying uncertainty levels and capturing most observed data within its prediction intervals. The predictive equation obtained from the model is easily interpretable for future studies.
- The applicability of the model was assessed in the first case study, demonstrating high accuracy in predicting the strength of stabilized soil specimens with different mixtures, highlighting the robustness of the model for various applications. However,

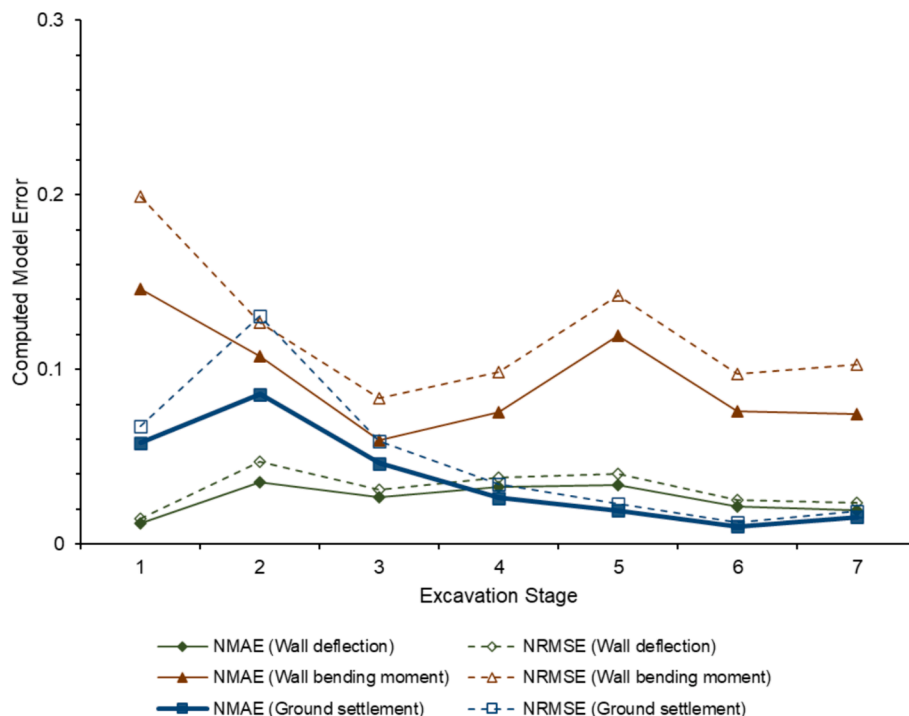


Fig. 11. Computed model error for each excavation stage for the estimation of ground and wall responses for TNEC, Taiwan.

caution is advised when generalizing the model to significantly different geomaterials due to potential high data variability.

- (c) The GBN model with sequential updating effectively evaluated soil-structure interactions in deep excavations. This technique, proven through an established case history, accurately estimated wall deflection, wall bending moment, and ground surface settlement profiles in deep excavations. The framework could sequentially update the model as excavations deepen, improving its performance by incorporating previously learned outcomes into subsequent stages. However, caution is necessary when applying it to excavations with significantly different geological conditions, due to insufficient model information for efficient learning of new soil parameter relationships.

CRedit authorship contribution statement

S.C. Jong: Writing – original draft, Visualization, Validation, Software, Methodology, Investigation, Formal analysis, Data curation. **D.E. L. Ong:** Writing – review & editing, Supervision, Project administration, Conceptualization.

Declaration of competing interest

The authors declare that they have no known competing financial interests or personal relationships that could have appeared to influence the work reported in this paper.

Data availability

Data will be made available on request.

Acknowledgements

This research did not receive any specific grant from funding agencies in the public, commercial, or not-for-profit sectors.

Appendix A. Supplementary Material

Supplementary material to this article can be found online at <https://doi.org/10.1016/j.compgeo.2024.106452>.

References

- Bentley Systems. PLAXIS 2D: 2D geotechnical engineering software 2022.
- Betancourt, M., 2017. A conceptual introduction to Hamiltonian Monte Carlo. *ArXiv Methodol.*
- Cheng, W.C., Li, G., Ong, D.E.L., Chen, S.L., Ni, J.C., 2020. Modelling liner forces response to very close-proximity tunnelling in soft alluvial deposits. *Tunn. Undergr. Sp. Technol.* 103, 103455 <https://doi.org/10.1016/j.tust.2020.103455>.
- Ching, J., Phoon, K.K., 2019. Constructing site-specific multivariate probability distribution model using Bayesian machine learning. *J. Eng. Mech.* 145, 1–15. [https://doi.org/10.1061/\(ASCE\)EM.1943-7889.0001537](https://doi.org/10.1061/(ASCE)EM.1943-7889.0001537).
- Ching, J., Lin, G.H., Phoon, K.K., Chen, J., 2017. Correlations among some parameters of coarse-grained soils — the multivariate probability distribution model. *Can. Geotech. J.* 54, 1203–1220. <https://doi.org/10.1139/cgj-2016-0571>.
- Chong, E.E.M., 2020. Soil-structure interaction due to adjacent deep excavation considering groundwater drawdown and presence of capping beam. PhD thesis. Swinburne University of Technology.
- Clough, G.W., O'Rourke, T.D., 1990. Construction induced movements of insitu walls. *Spec. Conf. Des. Perform. Earth Retain. Struct.* 439–470.
- Duane, S., Kennedy, A.D., Pendleton, B.J., Roweth, D., 1987. Hybrid Monte Carlo. *Phys. Lett. B* 195, 216–222. [https://doi.org/10.1016/0370-2693\(87\)91197-X](https://doi.org/10.1016/0370-2693(87)91197-X).
- Elbaz, K., Shen, S.L., Zhou, A., Yuan, D.J., Xu, Y.S., 2019. Optimization of EPB shield performance with adaptive neuro-fuzzy inference system and genetic algorithm. *Appl. Sci.* 9, 780. <https://doi.org/10.3390/app9040780>.
- Gabry, J., Mahr, T., 2021. bayesplot: Plotting for Bayesian Models.
- Gelman, A., Goodrich, B., Gabry, J., Vehtari, A., 2019. R-squared for Bayesian regression models. *Am. Stat.* 73, 307–309. <https://doi.org/10.1080/00031305.2018.1549100>.
- Geyer, C.J., 1992. Practical Markov chain Monte Carlo. *Stat. Sci.* 7, 473–483. <https://doi.org/10.1214/ss/1177011137>.
- Ghasemi, E., Gholizadeh, H., 2019. Prediction of squeezing potential in tunneling projects using data mining-based techniques. *Geotech. Geol. Eng.* 37, 1523–1532. <https://doi.org/10.1007/s10706-018-0705-6>.
- Gong, W., Tien, Y.M., Juang, C.H., Martin, J.R., Luo, Z., 2017. Optimization of site investigation program for improved statistical characterization of geotechnical property based on random field theory. *Bull. Eng. Geol. Environ.* 76, 1021–1035. <https://doi.org/10.1007/s10064-016-0869-3>.
- Goodrich, B., Gabry, J., Ali, I., Brilleman, R., Stanarm, S., 2020. Bayesian Applied Regression Modeling via Stan.
- Horpibulsuk, S., Rachan, R., Chinkulkijniwat, A., Raksachon, Y., Suddepong, A., 2010. Analysis of strength development in cement-stabilized silty clay from microstructural considerations. *Constr. Build. Mater.* 24, 2011–2021. <https://doi.org/10.1016/j.conbuildmat.2010.03.011>.
- Houlsby, N.M.T., Houlsby, G.T., 2013. Statistical fitting of undrained strength data. *Geotechnique* 63, 1253–1263. <https://doi.org/10.1680/geot.13.P.007>.
- Hsieh, P.G., Ou, C.Y., 1998. Shape of ground surface settlement profiles caused by excavation. *Can. Geotech. J.* 35, 1004–1017. <https://doi.org/10.1139/t98-056>.
- Hu, Y., Wang, Y., Zhao, T., Phoon, K.K., 2020. Bayesian supervised learning of site-specific geotechnical spatial variability from sparse measurements. *ASCE-ASME J. Risk Uncertain. Eng. Syst. Part A Civ. Eng.* 6, 1–12. <https://doi.org/10.1061/AJRUA6.0001059>.
- Hu, Y., Wang, Y., 2020. Probabilistic soil classification and stratification in a vertical cross-section from limited cone penetration tests using random field and Monte Carlo simulation. *Comput. Geotech.* 124, 103634 <https://doi.org/10.1016/j.compgeo.2020.103634>.
- Jin, Y., Biscontin, G., Gardoni, P., 2018. A Bayesian definition of 'most probable' parameters. *Geotech. Res.* 5, 130–142. <https://doi.org/10.1680/jgere.18.00027>.
- Jin, Y.F., Yin, Z.Y., Zhou, W.H., Shao, J.F., 2019. Bayesian model selection for sand with generalization ability evaluation. *Int. J. Numer. Anal. Methods Geomech.* 43, 2305–2327. <https://doi.org/10.1002/nag.2979>.
- Joaquin. SoilStabilityBishop Method RoibalME540 2024.
- Johnson, A.A., Ott, M.Q., Dogucu, M., 2021. Bayes Rules! An Introduction to Applied Bayesian Modeling.
- Jong, S.C., Ong, D.E.L., Oh, E., 2021. State-of-the-art review of geotechnical-driven artificial intelligence techniques in underground soil-structure interaction. *Tunn. Undergr. Sp. Technol.* 113, 10.1016/j.tust.2021.103946.
- Jong, S.C., Ong, D.E.L., Oh, E., 2022. A novel Bayesian inference method for predicting optimum strength gain in sustainable geomaterials for greener construction. *Constr. Build. Mater.* 344, 128255.
- Khalaj, S., BahooToroody, F., Mahdi Abaei, M., BahooToroody, A., De Carlo, F., Abbassi, R., 2020. A methodology for uncertainty analysis of landslides triggered by an earthquake. *Comput. Geotech.* 117, 103262 <https://doi.org/10.1016/j.compgeo.2019.103262>.
- Korff, M., 2013. Response of piled buildings to the construction of deep excavations. PhD thesis. University of Cambridge, 10.3233/978-1-61499-274-5-i.
- Koski, T., Noble, J.M., 2009. Bayesian Networks: An Introduction. John Wiley & Sons, 10.3233/978-1-61499-274-5-i.
- Kung, G.T.C., Ou, C.Y., Juang, C.H., 2009. Modeling small-strain behavior of Taipei clays for finite element analysis of braced excavations. *Comput. Geotech.* 36, 304–319. <https://doi.org/10.1016/j.compgeo.2008.01.007>.
- Kurnaz, T.F., Kaya, Y., 2018. The comparison of the performance of ELM, BRNN, and SVM methods for the prediction of compression index of clays. *Arab. J. Geosci.* 11, 770. <https://doi.org/10.1007/s12517-018-4143-9>.
- Leong, H.Y., Ong, D.E.L., Sanjayan, J.G., Nazari, A., 2015. A genetic programming predictive model for parametric study of factors affecting strength of geopolymers. *RSC Adv.* 5, 85630–85639. <https://doi.org/10.1039/c5ra16286f>.
- Likitersuang, S., Chheng, C., Keawsawavong, S., 2019. Structural modelling in finite element analysis of deep excavation. *J. Geoenviron. Eng.* 14, 121–128. [https://doi.org/10.6310/jog.201909_14\(3\).1](https://doi.org/10.6310/jog.201909_14(3).1).
- Lim, A., Ou, C.Y., 2017. Stress paths in deep excavations under undrained conditions and its influence on deformation analysis. *Tunn. Undergr. Sp. Technol.* 63, 118–132. <https://doi.org/10.1016/j.tust.2016.12.013>.
- Liu, Y., Ong, D.E.L., Oh, E., Liu, Z., Hughes, R., 2022. Sustainable cementitious blends for strength enhancement of dredged mud in Queensland, Australia. *Geotech. Res.* <https://doi.org/10.1680/jgere.21.00046>.
- Masters, T., 1993. Practical Neural Networks Recipes in C++.
- Mehdizadeh, A., Disfani, M.M., Evans, R., Arulrajah, A., Ong, D.E.L., 2015. Discussion of "development of an internal camera-based volume determination system for triaxial testing" by S. E. Salazar, A. Barnes, and R. A. Coffman. The technical note was published in *Geotechnical Testing Journal*, Vol. 38, No. 4, 2015. [DOI: 10.1520/Geotech Test J 2016;39:165–8. 10.1520/GTJ20150153].
- Murphy, K.P., 2012. Machine Learning: A Probabilistic Perspective. MIT Press.
- Neal, R.M., 2011. MCMC using Hamiltonian dynamics. In: Brooks, S., Gelman, A., Jones, G.L., Meng, X.L. (Eds.), *Handb. CRC Press, Markov Chain Monte Carlo*, pp. 113–162.
- Omeregic, A.I., Palombo, E.A., Ong, D.E.L., Nissom, P.M., 2019. Biocementation of sand by *Sporosarcina pasteurii* strain and technical-grade cementation reagents through surface percolation treatment method. *Constr. Build. Mater.* 228, 116828 <https://doi.org/10.1016/j.conbuildmat.2019.116828>.
- Ong, D.E.L., 2004. Pile behaviour subject to excavation-induced soil movement in clay. PhD thesis. National University of Singapore.
- Ong, D.E.L., Yang, D.Q., Phang, S.K., 2006. Comparisons of finite element modelling of a deep excavation using SAGE-CRISP and PLAXIS. In: *Proc. Int. Conf. Deep Excav., Singapore: International Conference on Deep Excavations*, pp. 51–64.
- Ou, C.Y., Liao, J.T., Cheng, W.L., 2000. Building response and ground movements induced by a deep excavation. *Geotechnique* 50, 209–220. <https://doi.org/10.1680/geot.2000.50.3.209>.

- Pham, V., Oh, E., Ong, D.E.L., 2021. Gene-expression programming-based model for estimating the compressive strength of cement-fly ash stabilized soil and parametric study. *Infrastructures* 6, 181. <https://doi.org/10.3390/infrastructures6120181>.
- Pham, V., Oh, E., Ong, D.E.L., 2022. Effects of binder types and other significant variables on the unconfined compressive strength of chemical-stabilized clayey soil using gene-expression programming. *Neural Comput. Appl.* <https://doi.org/10.1007/s00521-022-06931-0>.
- Phoon, K.K., Ching, J., 2014. Risk and reliability in geotechnical. *Engineering*. <https://doi.org/10.1201/b17970>.
- PLAXIS 2D Material Models Manual. PLAXIS 2D Material Models Manual 2022.
- Qi, X.H., Zhou, W.H., 2017. An efficient probabilistic back-analysis method for braced excavations using wall deflection data at multiple points. *Comput. Geotech.* 85, 186–198. <https://doi.org/10.1016/j.compgeo.2016.12.032>.
- R Core Team. R: A Language and Environment for Statistical Computing 2021.
- RStudio Team. RStudio: Integrated Development Environment for R 2021.
- Schanz, T., Vermeer, P.A., Bonnier, P.G., 2000. The hardening soil model: Formulation and verification. *Beyond 2000 Comput. Geotech. Ten Years PLAXIS In: Int. Proc. Int. Symp. Amsterdam, March 1999*, Balkema, Rotterdam: 1999. 10.1201/9781315138206-27.
- Scutari, M., 2010. Learning Bayesian networks with the bnlearn R Package. *J. Stat. Softw.* 35 (1–22). <https://doi.org/10.18637/jss.v035.i03>.
- Scutari, M., Denis, J.-B., 2014. *Bayesian Networks: With Examples in R*. Taylor & Francis, Boca Raton.
- Shams, R., 2024. SPT Value correction for Dilatancy.
- Shi, C., Wang, Y., 2021. Non-parametric machine learning methods for interpolation of spatially varying non-stationary and non-Gaussian geotechnical properties. *Geosci. Front.* 12, 339–350. <https://doi.org/10.1016/j.gsf.2020.01.011>.
- Stuyts, B., 2020. Groundhog: a general-purpose Python library for geotechnical engineering.
- Walker, R., 2018. geotechnica: A software suite for geotechnical engineering.
- Wang, Y., Cao, Z., 2013. Probabilistic characterization of Young's modulus of soil using equivalent samples. *Eng. Geol.* 159, 106–118. <https://doi.org/10.1016/j.enggeo.2013.03.017>.
- Wang, Y., Zhao, T., 2017. Bayesian assessment of site-specific performance of geotechnical design charts with unknown model uncertainty. *Int. J. Numer. Anal. Methods Geomech.* 41, 781–800. <https://doi.org/10.1002/nag.2658>.
- Wickham, H., 2016. ggplot2: Elegant Graphics for Data Analysis.
- Yang, L., Feng, X., Sun, Y., 2019. Predicting the Young's modulus of granites using the Bayesian model selection approach. *Bull. Eng. Geol. Environ.* 78, 3413–3423. <https://doi.org/10.1007/s10064-018-1326-2>.
- Zhao, L.-S., Zhou, W.-H., Su, L.-J., Garg, A., Yuen, K.-V., 2019. Selection of physical and chemical properties of natural fibers for predicting soil reinforcement. *J. Mater. Civ. Eng.* 31, 04019212. [https://doi.org/10.1061/\(asce\)mt.1943-5533.0002850](https://doi.org/10.1061/(asce)mt.1943-5533.0002850).